

# *Albino midrib 1*, encoding a putative potassium efflux antiporter, affects chloroplast development and drought tolerance in rice

Peike Sheng · Junjie Tan · Mingna Jin · Fuqing Wu · Kunneng Zhou · Weiwei Ma · Yueqin Heng · Jiulin Wang · Xiuping Guo · Xin Zhang · Zhijun Cheng · Linglong Liu · Chunming Wang · Xuanming Liu · Jianmin Wan

Received: 6 March 2014/Revised: 17 May 2014/Accepted: 26 May 2014/Published online: 11 June 2014  
© Springer-Verlag Berlin Heidelberg 2014

## Abstract

**Key message** Mutation of the *AMI* gene causes an albino midrib phenotype and enhances tolerance to drought in rice

**Abstract**  $K^+$  efflux antiporter (KEA) genes encode putative potassium efflux antiporters that are mainly located in plastid-containing organisms, ranging from lower green algae to higher flowering plants. However, little genetic evidence has been provided on the functions of KEA in chloroplast development. In this study, we isolated a rice mutant, *albino midrib 1* (*aml1*), with green- and white-variegation in the first few leaves, and albino midrib phenotype in older tissues. We found that *AMI* encoded a

putative KEA in chloroplast. *AMI* was highly expressed in leaves, while lowly in roots. Chloroplast gene expression and proteins accumulation were affected during chlorophyll biosynthesis and photosynthesis in *aml1* mutants. Interestingly, *AMI* was induced by salt and PEG, and *aml1* showed enhanced sensitivity to salinity in seed germination and increased tolerance to drought. Taken together, we concluded that KEAs were involved in chloroplast development and played important roles in drought tolerance.

**Keywords** KEA · Rice (*Oryza sativa* L.) · Chloroplast · Drought tolerance · *AMI* gene

## Abbreviations

Car	Carotenoid
Chl	Chlorophyll
KEA	Potassium ( $K^+$ ) efflux antiporter
ORF	Open reading frame
DAB	Diaminobenzidine
GFP	Green fluorescent protein

Communicated by Jeong Sheop Shin.

P. Sheng and J. Tan contributed equally to this work.

**Electronic supplementary material** The online version of this article (doi:10.1007/s00299-014-1639-y) contains supplementary material, which is available to authorized users.

P. Sheng · J. Tan · X. Liu  
State Key Laboratory of Chemo/Biosensing and Chemometrics,  
College of Biology, Hunan University,  
Changsha 410082, Hunan, China

P. Sheng · J. Tan · M. Jin · F. Wu · K. Zhou · W. Ma ·  
Y. Heng · J. Wang · X. Guo · X. Zhang · Z. Cheng ·  
J. Wan (✉)  
National Key Facility for Crop Gene Resources and Genetic  
Improvement, Institute of Crop Science, Chinese Academy  
of Agricultural Sciences, Beijing 100081, China  
e-mail: wanjianmin@caas.cn; wanjm@njau.edu.cn

L. Liu · C. Wang · J. Wan  
National Key Laboratory for Crop Genetics and Germplasm  
Enhancement, Nanjing Agricultural University,  
Nanjing 210095, Jiangsu, China

## Introduction

Rice is one of the most important crops in the world. Photosynthesis, as a resource for energy in plants, is closely related to crops yield. Chloroplasts, where photosynthesis occurs, play essential roles not only in photoautotrophic growth but also in transduction of stress-associated signals. Most of chloroplast proteins (>80 %) are encoded within the nucleus and imported into the chloroplast after translation in the cytosol (Rodermel 2001). In rice, nuclear genes modulating chloroplast development have been largely studied. Mutations of them

often cause the abnormal coloration from the seedling stage (Archer and Bonnett 1987).

Chlorophyll-deficient mutants are ideal genetic materials to gain insight into molecular mechanisms that modulate chlorophyll biosynthesis and chloroplast development in plants. To date, a considerable number of such mutants have been discovered in rice. Based on phenotypes, they were referred to as albino, pale-green chlorine (yellow), stripe and zebra (Jung et al. 2003). Almost all of known gene loci involved in these mutations were located to the chromosomes, and many have been cloned and characterized (Zhou et al. 2013; Dong et al. 2013; Su et al. 2012; Kusumi et al. 2011; Yoo et al. 2009; Sugimoto et al. 2004, 2007; Zhang et al. 2006; Song et al. 2004; Jung et al. 2003). However, few have been reported to associate with abiotic stresses.

The  $K^+$  efflux antiporters (KEAs) comprised a new family originated from bacterial glutathione-regulated  $K^+$  efflux transporters KefB and KefC with an N-terminal  $Na^+$  exchanger domain and a C-terminal KTN-NAD (H)-binding domain (also called TrkA\_N domain) (Chanroj et al. 2012; Choe 2002). The KEA family was categorized into three types: KEA Ia, KEA Ib and KEA II (Chanroj et al. 2012). KEA Ia and KEA Ib contain a C-terminal KTN domain which is lost in the KEA II. Clades Ia and Ib can be distinguished by its N-terminal domain. Clades Ia has a long hydrophilic N-terminal domain of about 570–770 amino acids, while clades Ib does not have and its C-terminus is slightly longer than the other sequence (Chanroj et al. 2012). The KEA genes in higher plants were firstly reported and classified in the *Arabidopsis thaliana* (Maser et al. 2001), where KEA genes could be divided into two main branches with AtKEA1–3 and AtKEA4–6. AtKEA1–3 harbored a complete C-terminal KTN domain and was closely related to bacterial EcKefB and EcKefC-like proteins (Booth 2003), and AtKEA4–6 had lost the KTN domain in the C-terminus and shared the high homology to cyanobacterial sequences, similar to the TMCO3-like proteins from metazoan (Chanroj et al. 2012).

To date, little information is available on the function of KEAs in plants. Only a member of KEA family from *Arabidopsis* has been functionally characterized. AtKEA2, a homolog of bacterial KefC, encodes a  $K^+/H^+$  antiporter and the truncated AtKEA2 (AtsKEA2) lacking the N-terminal domain can well complement disruption of the  $Na^+(K^+)/H^+$  antiporter Nhx1p to confer hygromycin resistance and tolerance to  $Na^+$  or  $K^+$  stress and mediated cation/ $H^+$  exchange with preference for  $K^+ = Cs^+ > Li^+ > Na^+$  in yeast (Aranda-Sicilia et al. 2012). Additionally, the AtKEA2 was predicted to have a chloroplast transit peptide which was confirmed by subcellular localization, suggesting its functions in chloroplast or plastids development (Aranda-Sicilia et al. 2012). However, no

genetic evidence with any relative KEA mutants is reported to support this hypothesis.

In this paper, we isolated and characterized the first KEA mutant *aml* with a chlorophyll-deficient phenotype in the leaves by map-based cloning in rice. Abnormal chloroplast gene expression and protein accumulation in *aml* suggested the crucial function of KEA in chloroplast development. In addition, *aml* enhanced drought tolerance as compared to wild-type. Our findings revealed that the KEAs played important roles in tolerance to abiotic stresses in rice.

## Materials and methods

### Plant materials and growth conditions

The rice *albino midrib* (*aml*) mutant was isolated from a  $^{60}Co$ -irradiated mutant pool of japonica rice cultivar *Wu B*. The *aml* was crossed with *Jin 23B* and *Pei'ai64* to construct the F<sub>2</sub> population for mapping. Rice plants were grown in a paddy field in Beijing (39°54'N, summer season, temperate climate) and Hainan (18°16'N, winter season, subtropical climate) under local conditions or in a growth chamber. For the temperature treatments, seedlings were planted in a growth chamber under 12 h of light/12 h of dark at a constant 30 or 20 °C.

### Chlorophyll and carotenoid content measurement

Chlorophyll and carotenoid contents were measured using a spectrophotometer according to the method described by (Arnon 1949). Briefly, leaves (approximately 0.2 g FW) were cut and marinated in 95 % ethanol for 24 h under dark conditions. The supernatants were collected by centrifugation and analyzed with a Spectrophotometer (Beckman Coulter DU-800, USA) at 665, 649 and 470 nm, respectively.

### Transmission electron microscopy

Samples of wild-type and *aml* mutant leaves were fixed in 2.5 % glutaraldehyde at 4 °C for 4 h, rinsed and incubated overnight in 1 % OsO<sub>4</sub> at 4 °C, dehydrated using an ethanol series, and finally embedded in Spurr's medium prior to thin sectioning. Samples were stained again with uranylacetate and examined with a Hitachi H-7650 transmission electron microscope.

### Mapping and cloning of *AMI*

For mapping *AMI*, a cross was made between *aml* mutant and an indica cultivar PA 64. Firstly, the F<sub>2</sub> population of

ten individuals with typical *aml* mutant phenotype was used for linkage analysis, then 882 F2 plants with *aml* mutant phenotypes for fine-mapping. Sequence polymorphisms between Nipponbare (japonica) and 93-11 (indica) were identified and used to develop molecular markers. Primer pairs were designed using the Web server program dCAPS Finder 2.0 (<http://helix.wustl.edu/dcaps/dcaps.html>). The PCR procedure was as follows: 95 °C for 5 min, followed by 34 cycles of 95 °C for 30 s, 58 °C for 30 s, 72 °C for 40 s, and a final elongation step at 72 °C for 5 min.

#### Complementation of the *aml* mutant

For complementation of the *AMI* mutation, a 6.4 kb DNA fragment containing the entire CDS of *AMI* and a 2.8 kb upstream sequence was amplified by PCR from *Wu B*, respectively, and then cloned into the binary vector pCAMBIA1305. The constructs were introduced into *aml* mutant by *Agrobacterium tumefaciens*-mediated transformation as described previously (Hiei et al. 1994).

#### Sequence and phylogenetic analysis

Gene prediction and structure analysis were performed using the GRAMENE database (<http://www.gramene.org/>). Homologous sequences of *AMI* were identified using the Blastp search program of the National Center for Biotechnology Information (NCBI, <http://www.ncbi.nlm.nih.gov/>). Multiple sequence alignments were conducted with DNAMAN version 6.0 (Lynnon Biosoft). The chloroplast transit peptide (CTP) was predicted by the ChloroP program. PCR primers were designed with the Primer premier 5.0 software. A phylogenetic tree was constructed using MEGA v4.1 software (<http://www.megasoftware.net/>).

#### RNA preparation and qRT-PCR analysis

Total rice RNA was extracted with an RNA prep pure kit (Zymo Research, Orange, CA) according to the manufacturer's instructions. The first-strand cDNA was synthesized from 2 µg of total RNA using the SuperScript II kit (TaKaRa). Primer pairs (suppl Table S3) were designed using Primer Express (Applied Biosystems) and listed in. qRT-PCR was conducted using an ABI7500 fast system with the SYBR Premix Ex Taq (TaKaRa; RR041A). The procedure was as follows: initial polymerase activation for 30 s at 95 °C followed by 40 cycles of 95 °C for 5 s and 60 °C for 34 s. For each sample, qRT-PCR was performed with three technical replicates on three biological replicates. The  $2^{-\Delta\Delta C_T}$  method was used to analyze relative transcript levels in gene expression.

#### Subcellular localization of AM1-GFP proteins in rice protoplasts

The coding sequence of *AMI* was amplified and cloned into the N-terminus of GFP under control of the CaMV 35S promoter in the transient expression vector pAN580-GFP, resulting in pAN580-*AMI*-GFP. The recombinant vector was then transformed into rice protoplasts according to protocols described previously (Chen et al. 2006). GFP fluorescence in the transformed protoplasts was visualized using a confocal laser-scanning microscope (LSM 700; Carl Zeiss, Germany).

#### Histochemical GUS assay and DAB staining

A putative 2.7 kb promoter genomic fragment upstream of the ATG start codon was amplified by PCR, and the PCR product was cloned into the binary vector pCAMBIA1305 to generate the transformation plasmid *pproAMI::GUS*. GUS histochemical assays were performed as described previously (Zhou et al. 2013). The stained tissues were photographed using a Canon camera (50D) and enhanced using Photoshop CS6 (Adobe).

H<sub>2</sub>O<sub>2</sub> was detected by DAB staining as described previously (Thordal-Christensen et al. 1997). The leaves from wild-type and *aml* plants were detached and vacuum-infiltrated with the DAB solution (1 mg of DAB dissolved in 1 ml of distilled water, pH 3.8). The leaves were placed in a growth chamber for 24 h at 25 °C and cleared in boiling ethanol (96 %) for 10 min before photographing.

#### Protein extraction, SDS-PAGE and western blotting

Leaf material was homogenized in lysis buffer [25 mM Tris-HCl, pH 7.6, 0.15 M NaCl, and 2 % sodium dodecyl sulfate (SDS), 0.01 % 2-mercaptoethanol]. Sample amounts were standardized by fresh weight. The protein samples were separated by 10 % SDS-polyacrylamide gel electrophoresis (PAGE). After electrophoresis, the proteins were transferred onto a PVDF membrane (Millipore) and incubated with specific antibodies. The signals were detected using an ECL Plus Western Blotting Detection Kit (Thermo) and visualized by an imaging system (Chemidoc<sup>TM</sup>X-RS; Bio-Rad).

## Results

#### Phenotypic characterization of the *aml* mutant

In the paddy field, the *aml* mutant displayed green- and white-variegation in the first few leaves, and the variegation appeared to be randomly distributed on the surface of

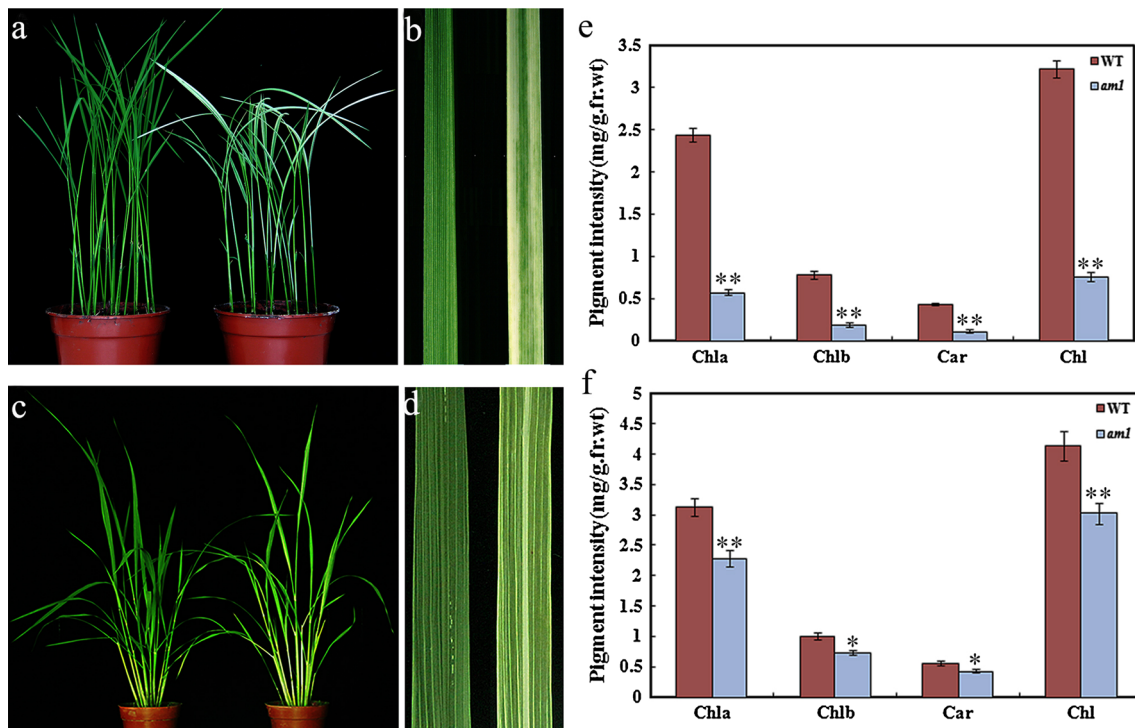


**Fig. 1** Phenotypic characteristics of wild-type (WT) and *aml* mutant. **a** 2-week-old wild-type (*left*) and *aml* (*right*) seedlings. **b** Enlarged views of the leaves from **a**. **c** 8-week-old wild-type (*left*) and *aml* (*right*) seedlings. **d** Enlarged views of the leaves from **c**. **e–f** The pigment contents in leaves of 2- and 8-week-old *aml* mutants are

much lower than that in wild-type. *Chla* chlorophyll *a*, *Chlb* chlorophyll *b*, *Chl* total chlorophyll, *Car* carotenoid. Data represents mean  $\pm$  SD from three independent biological replicates. Asterisks indicate statistically significant differences compared with wild-type (Student's *t* test: \* $P < 0.05$ ; \*\* $P < 0.01$ )

the mutant leaves and predominantly near the leaf margins (Fig. 1a, b). Approximately from the early tillering stage, the newly-grown leaves showed slightly yellow-green phenotype but in the leaf vein especially in midrib displayed albino (Fig. 1c, d). Consistent with the observations, the contents of chlorophyll and carotenoid in leaves of *aml* mutant were much lower than that of WT at the whole developmental stage (Fig. 1e, f). At maturity, the major agronomic traits such as plant height, number of tillers, and grain yield in *aml* plants were indistinguishable from those of wild-type plants (Table S1). Additionally, the degree of chlorosis in *aml* were strongly influenced by low temperature (such as 20 °C) (Fig. S1).

To investigate whether the mutation phenotype of the *aml* is associated with ultrastructure changes in the chloroplasts, we compared the ultrastructure of chloroplasts between white sectors of *aml* mutant leaves and wild-type normal leaves using transmission electron microscopy (TEM). As shown in Fig. 2, cells in WT leaves contained mature chloroplasts displaying well-organized lamellar structures and were equipped with normally stacked grana and thylakoid membranes. In contrast, cells of *aml* mutant contained abnormal plastids which were heretoplastic without any organized lamellar structures. These

observations revealed that the *AMI* mutation affected chloroplast development. Chloroplasts are the organelles in plant cells that perform photosynthesis. To test whether the photosynthetic apparatus was affected in *aml* mutants, we compared some key parameters between wild-type and *aml* plants using a pulse-amplitude-modulation (PAM) chlorophyll fluorometer. These parameters include photochemical efficiency of PSII ( $\Phi$ PSII), nonphotochemical quenching (NPQ, qN), photochemical quenching (qP, qL) and the maximal efficiency of PSII (Fv/Fm). These values were almost comparable between *aml* and wild-type plants (Table S2), indicating the PSII apparatus was not impaired in *aml* mutant.

#### Map-based cloning of *AMI* gene

Genetic analysis from the crosses *aml/Jin 32B* and *aml/Pei'ai64* indicated that the phenotype conferred by *aml* was caused by a single, recessive nuclear mutation (Table 1). Using F2 population from the cross between *aml* and *Pei'ai64*, the *AMI* locus was mapped on the long arm of chromosome 4, between markers W1 and W11 (Fig. 3a, b). Eleven insertion-deletion polymorphic (InDel) markers were designed between W1 and W11 (Table S3).

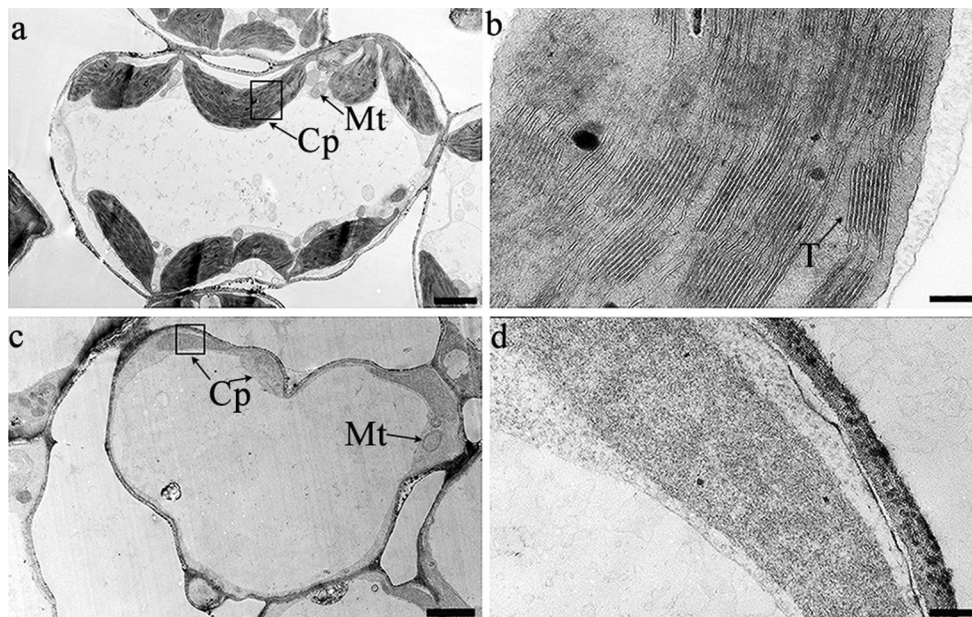


**Fig. 2** Observation of chloroplasts ultrastructure in mesophyll cells of 2-week-old wild-type and *am1* plants. **a, b** TEM illustrates the normal chloroplast ultrastructure in wild-type leaves by scale-up. **c, d** the *am1* mutant show the altered chloroplast ultrastructure in white

tissues compared with wild-type. The *black boxes* indicate the enlarged sections. *Cp* chloroplast, *Mt* mitochondria, *T* thylakoid lamellar. *Bars* = 2  $\mu$ m in **a** and **c**, 200 nm in **b** and **d**

**Table 1** Segregation for green and chlorosis seedlings in  $F_2$  populations from two crosses

Cross	<i>am1</i> /Jin 32B	<i>am1</i> /Pei'ai64
No. green plants	163	104
No. chlorosis plants	50	32
$\chi^2_{3:1}$ <sup>a</sup>	0.23	0.16

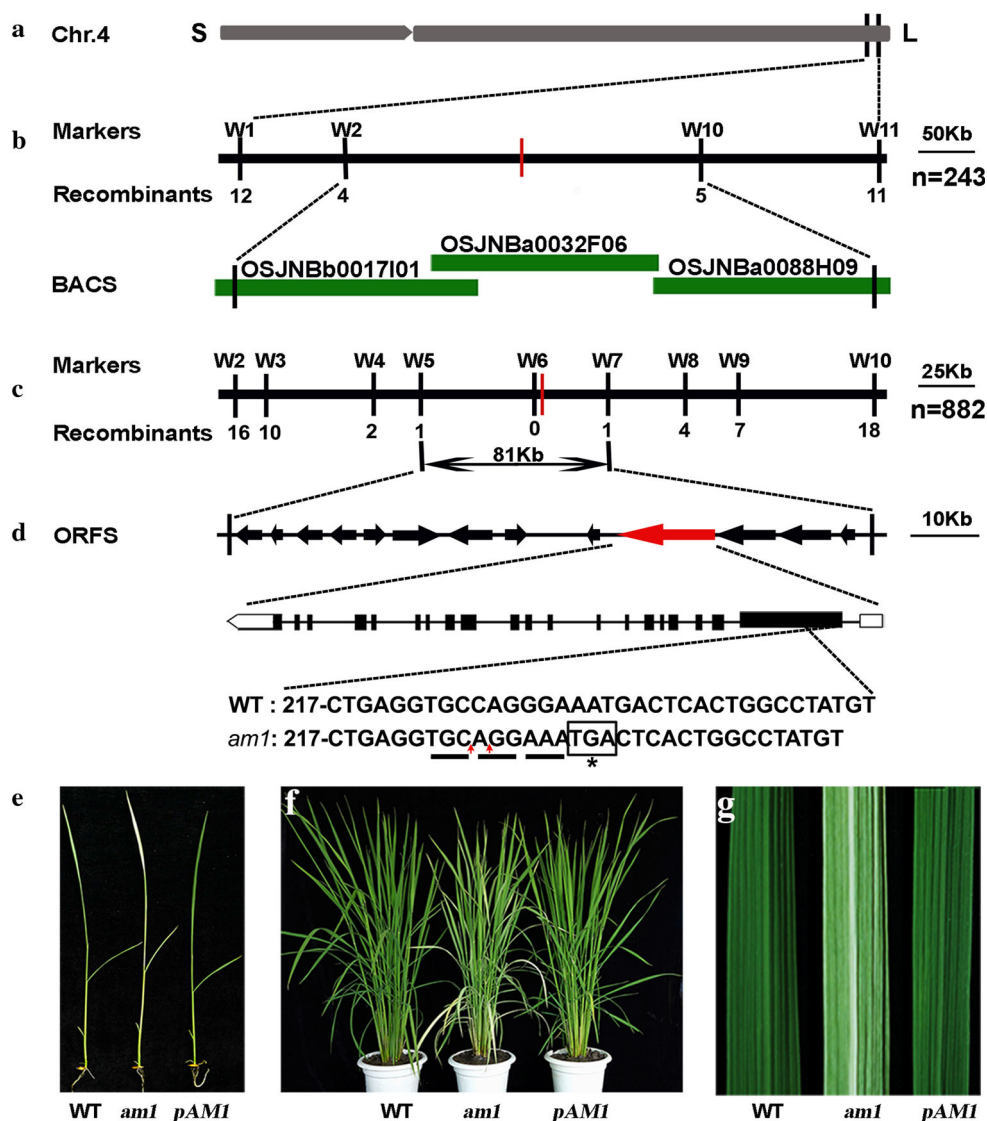
<sup>a</sup> Value for significance at  $P = 0.05$  and  $df = 3.84$

The *AM1* was further narrowed down to an 81 kb region between markers W5 and W7 (Fig. 3c) containing 13 putative ORFs (Fig. 3d). We sequenced all ORFs and only found a 2-bp deletion in the tenth ORF (LOC\_Os04g58620) at the position 226 and 228 bp away from the start codon ATG, causing a premature stop codon (Fig. 3d). We then introduced a 6.4-kb genomic fragment containing the transcriptional regulation elements and the full-length coding sequence of *AM1* into the *am1* mutant. As a result, all of 15 independent transgenic lines transformed with vector p*AM1* containing the wild-type LOC\_Os04g58620 gene completely rescued the mutant phenotype by comparing the leaf color of transgenic plants with wild-type plants and *am1* mutant (Fig. 3e–g). We failed to obtain the RNAi transgenic plants. The T0 generation transgenic seedlings all showed an albinism and were seedling-lethal (data not shown). Nevertheless, these results confirmed that LOC\_Os04g58620 corresponded to the *AM1* gene.

#### Sequence analysis of *AM1*

*AM1* was annotated in public databases (e.g., GRAMENE), as an encoding potassium efflux antiporter protein. *AM1* contained twenty exons and nineteen introns. The open reading frame (ORF) of *AM1* encodes a polypeptide of 1,155 amino acids with a calculated molecular mass of approximately 123 KD. Analysis of the *AM1* protein sequence by ChloroP (Emanuelsson et al. 1999); <http://www.cbs.dtu.dk/services/SignalP/>) suggested a 41 amino acid chloroplast transit peptide (CTP) in the N-terminus (Fig. 4a). By searching the *AM1* sequence against the Pfam database (Finn et al. 2010), two conserved domains were identified: one was Na<sup>+</sup>/H<sup>+</sup> Exchanger located between amino acids 553 and 928, and another TrkA\_N domain between amino acids 959 and 1,074 (Fig. 4a). Additionally, *AM1* protein possessed ten transmembrane domains (Fig. 4b). Based on these features, the *AM1* (LOC\_Os04g58620) was grouped into the KEA1a family (Chanroj et al. 2012). In this family, Arabidopsis KEA1 and KEA2 were previously reported. *AM1* shares very high peptide identity (65 %, 68 %) and similarity (76 %, 78 %) with both of KEA proteins (Fig. 4c). Phylogenetic tree analysis showed that *AM1* homologs were well differentiated and exhibited a clear evolutionary linkage from unicellular green algae to angiosperms. The homologs from algae to mosses formed a subclade, while the proteins from angiosperms formed a large subclade where those from monocots and dicots were clearly divided (Fig. S3). However,

**Fig. 3** Map-based cloning of the *AM1* gene. **a** The *AM1* locus was initially localized to the region between W1 and W11 markers in the chromosome 4 (Chr4). **b** Fine mapping of *AM1* which was spanned by BAC clones OSJNBb0017I01, OSJNBa0032F06 and OSJNBa0088H09. **c** The *AM1* locus was narrowed to a 81 kb region between the markers W5 and W7. The number of the recombinants identified from an F<sub>2</sub> population of 882 recessive phenotypes is shown below each marker. **d** The region contained 13 open reading frames (ORFs) and a 2 bp deletion (indicated by red arrow) in the ORF10, resulting in a frame-shift mutation. **e–g** Complementation of the *aml* mutant. The wild-type plants (left), *aml* mutants (middle), and mutants transformed with pAM1 vector (right) are shown (color figure online)



most of them were not functionally characterized except AtKEA2, mainly as a K<sup>+</sup>/H<sup>+</sup> antiporter (Aranda-Sicilia et al. 2012). Together, these findings suggested that AM1 functioned at the plastid membrane to control K<sup>+</sup>/H<sup>+</sup> exchange.

#### Subcellular localization of AM1

Prediction of CTP in the N-terminus of AM1 by ChloroP and the chlorophyll-deficient phenotype observed in the *aml* suggested a localization of AM1 in chloroplast. To examine the actual subcellular localization of AM1, an AM1-GFP construct was generated and then introduced into rice protoplasts by *A. tumefaciens* infiltration. Green fluorescent signals were visualized using confocal microscopy. Green fluorescent signals of AM1-GFP co-localized with the autofluorescent signals of chlorophyll

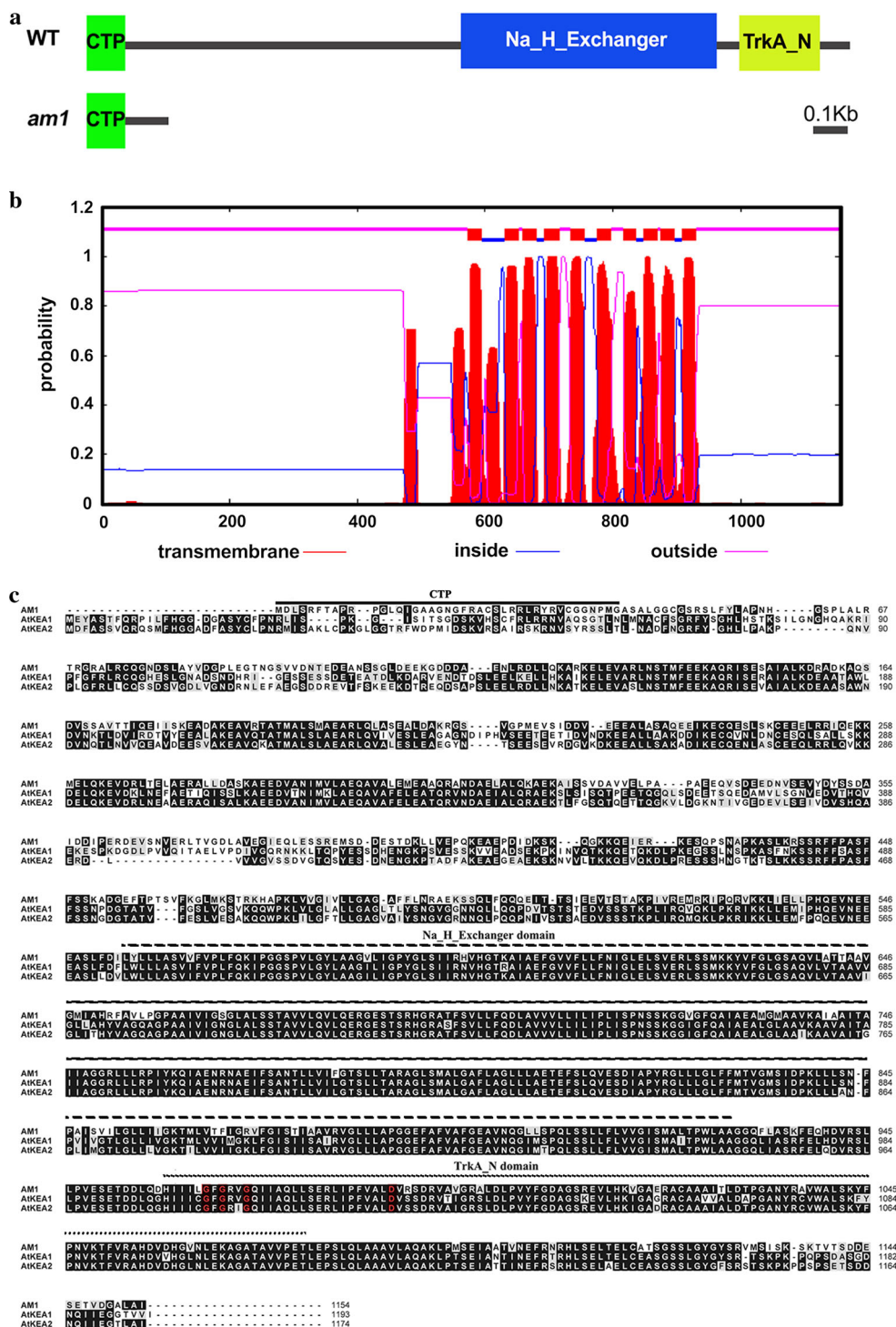
indicating that AM1 targeted the rice chloroplasts (Fig. 5a–d).

#### Expression analysis of AM1

Data submitted to the microarray transcript profiling database indicated that the *AM1* gene was widely expressed in rice, especially the leaves, throughout plant development ((Zimmermann et al. 2004); <https://www.genevestigator.ethz.ch>). To validate these data, we generated transgenic plants expressing a GUS reporter gene driven by the AM1 promoter (pAM1::GUS). Histochemical assay revealed that AM1 was highly expressed in the leaf, sheath, and panicle, while not in the root (Fig. 5e–i). This was confirmed by qRT-PCR using RNA samples from different parts of wild-type plants (Fig. 5j). We also analyzed *AM1* expression in different sections of leaves at

**Fig. 4** Sequence analysis of *AM1*. **a** The normal *AM1* protein contains three putative domains, including chloroplast transit peptides (CTP) in the N-terminal, Na<sub>2</sub>H<sub>2</sub>Exchanger domain and TrkA<sub>N</sub> domain, whereas the *am1* mutant protein only has CTP domain.

**b** Prediction of ten transmembrane helices of *AM1* protein by the program TMHMM available at <http://www.cbs.dtu.dk/services/TMHMM/>. **c** Alignment of *AM1* with *AtKEA1* and *AtKEA2*. Sequences are for *Oryza sativa* LOC\_Os04g58620 (*AM1*), *Arabidopsis thaliana* *AtKEA1* (AT1G01790.1) and *AtKEA2* (AT4G00630.2). Conserved amino acids are highlighted in shades of black. The predicted transit peptides, Na<sub>2</sub>H<sub>2</sub>Exchanger domain and KTN domains are labeled above the sequences by different lines. The Rossman fold motif is highlighted in red (color figure online)



various leaf developmental stages (Fig. 5k). We found that *AM1* was most highly expressed in the L3 section at the early chloroplast and leaf development stage (Fig. 5l). These results, together with chloroplast localization and the observed *am1* phenotype, supported that *AM1* played an important role in chloroplast development in rice leaves.

We next examined the transcription levels of the genes associated with chlorophyll biosynthesis, chloroplast development, or photosynthesis in the *am1* mutant. Nine genes were selected, including genes that encode Rubisco large subunit (*rbcL*; Hwang and Tabita 1989), glutamyl-tRNA reductase (*HEMA1*; Kumar and Soll 2000), NADPH: protochlorophyllide oxidoreductase A (*PORA*;

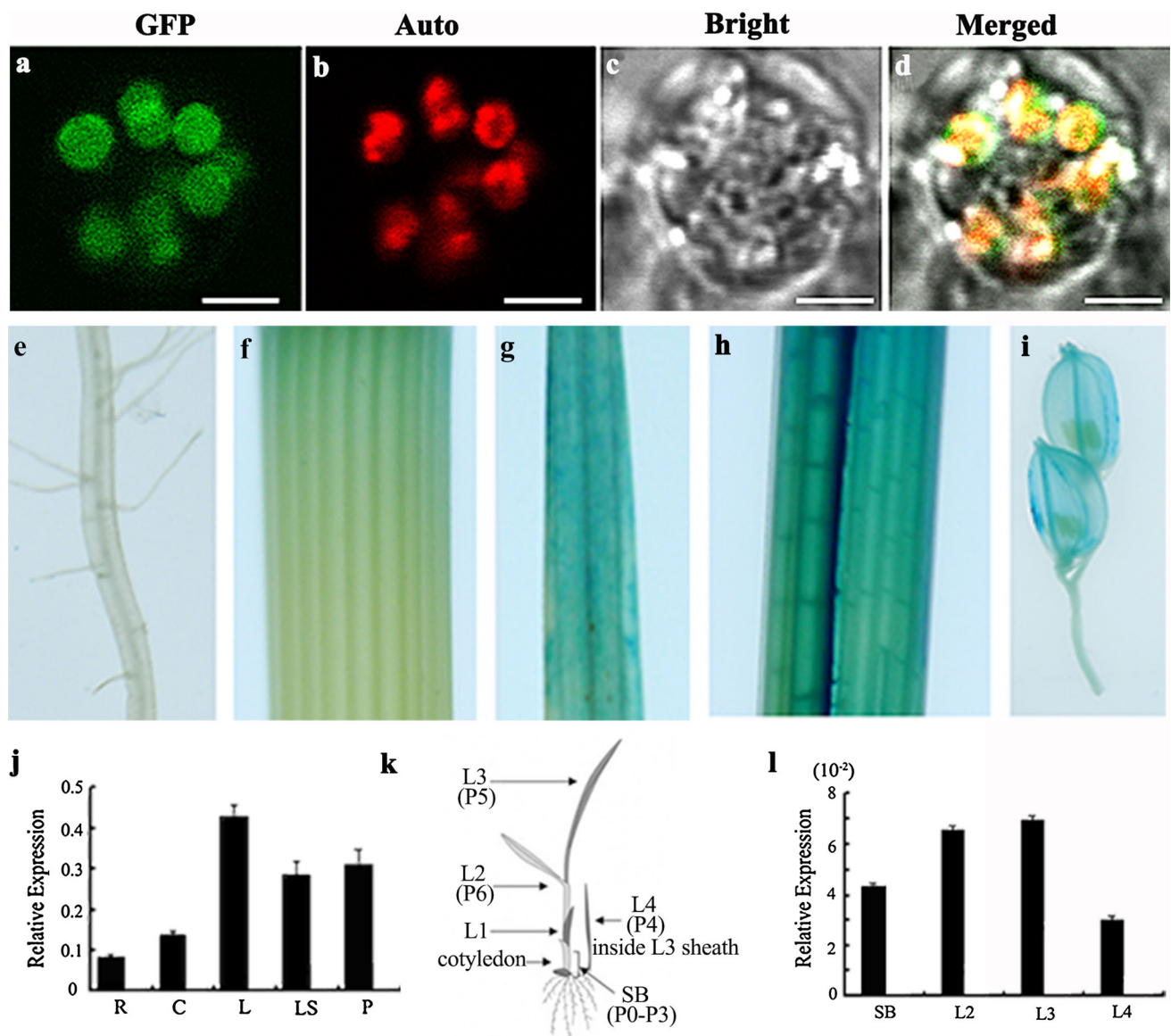


**Fig. 5** Subcellular localization and expression analysis of AM1. Subcellular localization of AM1. Fluorescence signals were detected by confocal microscopy. **a** Green fluorescence from AM1-GFP fusion protein. **b** Red fluorescence of chloroplast autofluorescence. **c** Bright-field image under transmitted light. **d** Merged image of **a**, **b** and **c**. Bars represent 5  $\mu$ m. **e–i** Histochemical staining shows that the p AM1::GUS reporter gene is ubiquitously expressed in roots, stems, leaves, leaf shoots, and panicles. **j** QRT-PCR analysis of AM1 in roots, stems, leaves, leaf shoots, and panicles of wild-type seedlings.

The means and SD were calculated from three independent experiments. **k** Schematic illustration of a rice seedling with fully expanded third leaf. *L1*, *L2*, *L3* and *L4* indicate the first, second, third and fourth leaves, respectively. Developmental stages (P0–P6) are also indicated. SB (shoot base) corresponds to a 5 mm piece from the bottom of the shoot and contains as yet unmerged leaves at the P0–P3 stages. **l** QRT-PCR analysis of AM1 in the SB, L2, L3 and L4 tissues of wild-type seedlings. The means and SD were calculated from three independent experiments

Holtorf and Apel 1996), light-harvesting Chl *a/b*-binding protein of PSII (CAB1R and CAB2R; Matsuoka 1990), YGL1 (Wu et al. 2007) and Mg-chelatase subunits (CHLD, CHLI and CHLH; Zhang et al. 2006). Most of these genes were all significantly down-regulated in the *am1* mutant except *YGL1* which was up-regulated in the mutant (Fig. 6a). These indicated that *AM1* played an important role in regulating the expression of genes associated with

chlorophyll biosynthesis, chloroplast development, and photosynthesis in the first few seedling leaves.

As the mutation affects chloroplast ultrastructure and chloroplast-associated gene expression, we examined the accumulation of photosynthetic proteins in the mutant. These proteins included photosystem-I subunits (PsaA), photosystem-II subunits (D1), the ATP synthase subunits (AtpA and AtpB), RNA polymerase subunits (RopB) and



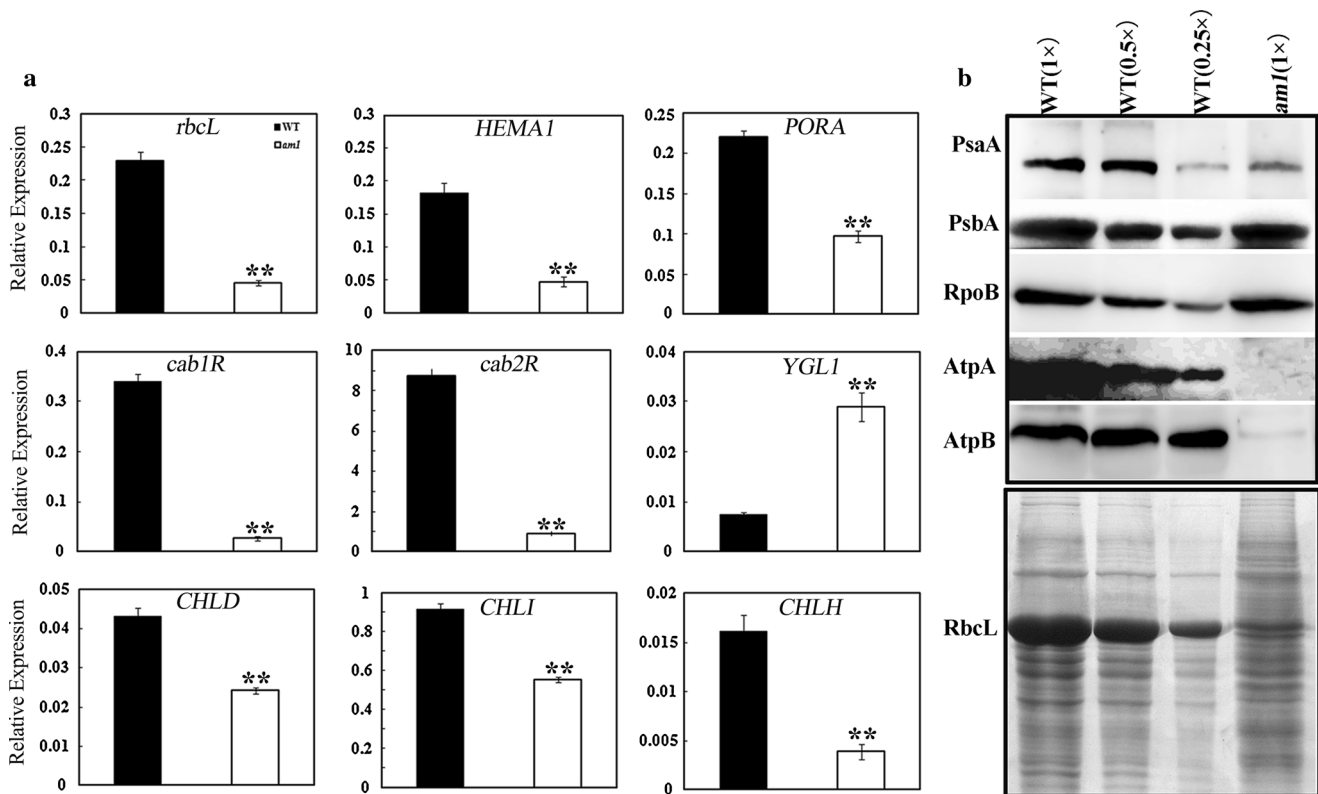


**Fig. 6** Analysis of gene transcription and protein accumulation associated with chlorophyll biosynthesis and photosynthesis in wild-type and *am1*. **a** Expression analysis of genes involved in chlorophyll biosynthesis, chloroplast development, or photosynthesis by QRT-PCR. Data represent mean  $\pm$  SD from three independent biological

replicates. Asterisks indicate statistically significant differences compared with wild-type (Student's *t* test:  $**P < 0.01$ ). **b** Western blot analysis of photosynthetic protein accumulation. The same filter was stained with Coomassie Brilliant Blue to visualize total proteins and the large subunit of Rubisco (RbcL) is indicated on the stained gel

the large subunit of soluble rubisco proteins (RbcL). The photosynthetic proteins AtpA and AtpB subunits were not detected in the *am1* mutants. The levels of *psaA* and RbcL were reduced in *am1* mutants compared with that of the wild-type. Meanwhile, the levels of *psbA* and RpoB were similar to those of the wild-type (Fig. 6b), indicating that the accumulation of most photosynthetic proteins was affected in *am1* mutants due to defective chloroplast development.

#### *Am1* show enhanced sensitivity to KCL at germination

Expression of *AMI* under various abiotic stresses and treatments was examined. As shown in Fig. 7a, *AMI* was induced under three treatments, including NaCl, KCl and drought (PEG treatment). PEG treatment led to earlier expression peak of *AMI* than salt treatments. Water and ABA treatments did not significantly alter *AMI* expression. Since *AMI* was predicted to be a potassium efflux antiporter (Fig. 4), we wondered whether *am1* altered responses to KCl. We examined the responses of *am1* mutant to added KCl at germination stage. Under the

normal condition, the *am1* mutant showed the similar germination rate to WT (Fig. 7b) but initiated germination with a 12 h delay relative to WT on MS medium supplemented with 100 mM KCl (Fig. 7c), and 24 h delay on medium with 200 mM KCl (Fig. 7d). These results suggested that *AMI* played an important role in potassium transport.

#### Enhanced tolerance to drought in *am1* mutant

Induction by PEG treatments suggested that *AMI* was likely involved in the drought tolerance. We investigated the effect of drought stress on the performance of *am1* plants. Four-week-old plants were analyzed. Under the normal conditions, *am1* plants grew normally and no significant differences were observed except for chlorosis. When water was withheld from these plants for 10 days, phenotypic changes were observed. WT plants exhibited severe symptoms of drought stress that the leaves became dry green, rolled and even withered; by contrast, these symptoms were substantially delayed in *am1* plants (Fig. 8a). We also summarized the survival rate of the WT

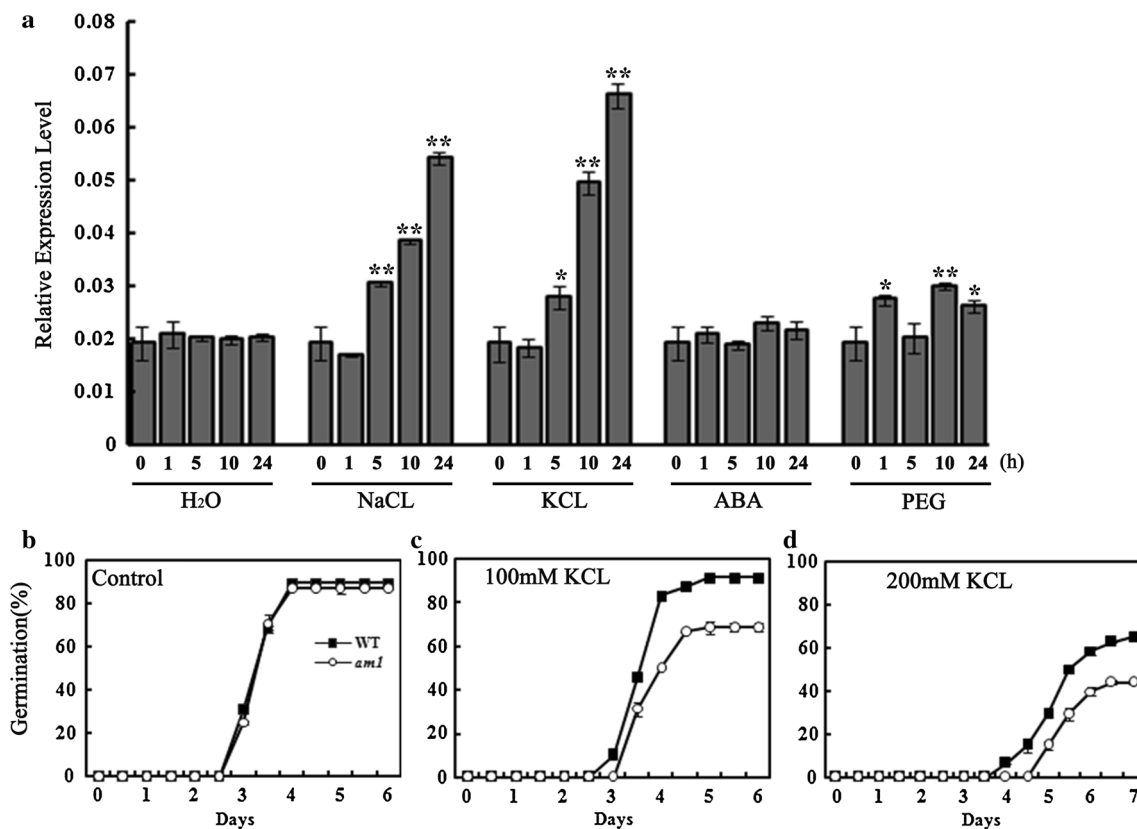


**Fig. 7** *Aml* show enhanced sensitivity to Kcl at germination. **a** Expression levels of *AM1* seedlings in response to Nacl, Kcl, ABA and PEG using qRT-PCR. Five-week-old wild-type seedlings were immersed with their roots in Nacl (200 mM), Kcl (200 mM), ABA (100  $\mu$ M), PEG (20 %) or H<sub>2</sub>O for the indicated times. After treatment, the aerial parts of seedlings were harvested and used for total RNA isolation. Germination rates of wild-type and *aml* seeds in

the absence (**b**), and presence of 100 mM (**c**), 200 mM (**d**) of Kcl. The germination was defined as the appearance of the white tip of the coleoptiles at least 5 mm long. Data represent mean  $\pm$  SD from three independent biological replicates. Asterisks indicate statistically significant differences compared with the control (Student's *t* test: \**P* < 0.05; \*\**P* < 0.01)

and *aml* plants after 12 days of watering; more than 67.5 % of *aml* plants recovered and grew normally whereas only about 12.5 % of WT plants recovered (Fig. 8b). These results indicated that *aml* could increase the tolerance to drought at the seedling stage.

Drought stress is known to be closely related to stomatal movements. We next examined the stomatal status in *aml* and WT plants. The 4-week-old WT and *aml* plants were exposed to drought stress for 1 week before they were used for stomatal analysis. As a result, 39.2 % of stomata were completely closed in the *aml* mutant plants, while only 19.8 % in the wild-type plants. At the mean time, only 11.3 % of stomata were completely open in the *aml* mutants, but 31.5 % in wild-type plants (Fig. 8c, d). The percentage of partially open stomata was similar in *aml* mutant and wild-type plants (48.6–50.2 %). These results showed that stomatal movement was greatly affected in *aml* mutants.

Since H<sub>2</sub>O<sub>2</sub> induces leaf stomatal closure (Huang et al. 2009; Bright et al. 2006; Apel and Hirt 2004; Hamilton

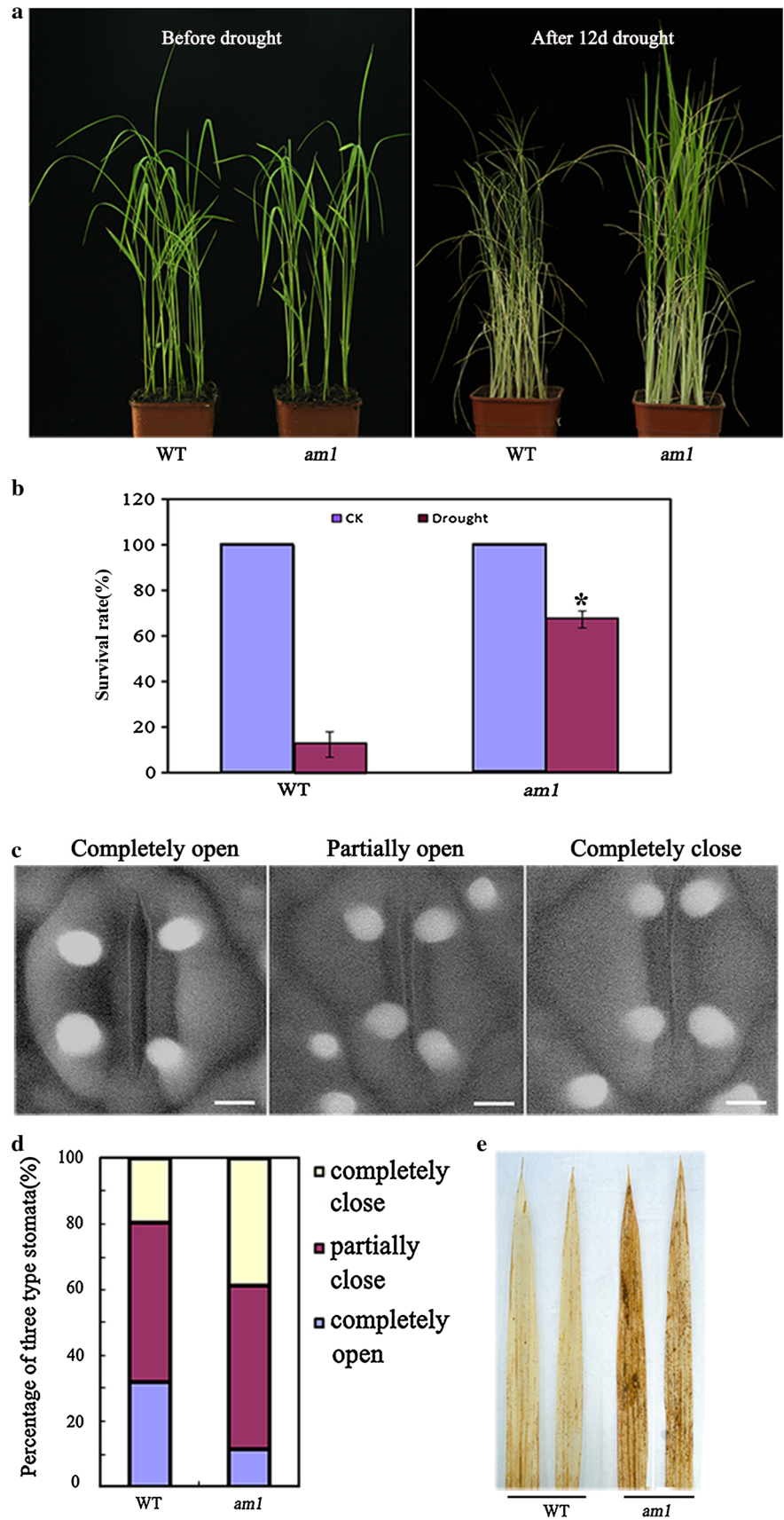
et al. 2000; McAinsh et al. 1996), we examined H<sub>2</sub>O<sub>2</sub> level in the wild-type and *aml* leaves by diaminobenzidine (DAB) staining and found a higher accumulation in *aml* mutant plants (Fig. 8e). These results suggested that accumulation of H<sub>2</sub>O<sub>2</sub> in *aml* mutants probably underlied the increased stomatal closure conferring the drought tolerance.

## Discussion

KEA genes encode putative K<sup>+</sup> efflux antiporters that are predominantly found in algae and plants but rarely in metazoan. In the current study, we isolated the first KEA mutant *aml* through map-based cloning in rice. The mutant allele displayed chlorophyll-deficient phenotype in the leaves suggesting an essential role in normal chloroplast development. In addition, *aml* showed enhanced drought tolerance as compared to WT. Thus, KEAs played important role in abiotic stress tolerance.

**Fig. 8** Enhanced tolerance to drought in *am1* mutant.

**a** Drought treatment of wild-type and *am1* mutant plants. Twenty-day-old plants were subjected to drought stress for 12 days. **b** Survival rate of the plants shown in **a** after 12 days of recovery from drought stress. All non-treated plants (CK) show 100 % survival. Data represent mean  $\pm$  SD from three replicates. *Asterisks* indicate statistically significant differences compared with the wild-type at  $P < 0.01$ . **c** Environmental scanning electron microscopy images of three levels of stomatal opening. *Bar* = 5  $\mu$ m. **d** The percentage of three levels of stomatal opening in wild-type and *am1* mutant ( $n = 78$  stomata for wild-type;  $n = 89$  stomata for *am1*). **e** DAB staining of the seedling leaves from wild-type and *am1* mutant



KEA proteins constitute an ancient group of transporters homologous with bacterial transporters harboring a C-terminal KTN domain, the presence of which is a feature shared by most of bacterial  $K^+$  channels and transporters such as Kch, TrkA, Ybal, and KefB or KefC (Choe 2002). Its minimal functional unit is a dimeric molecule connected by a flexible hinge. Hinge move can be physically coupled with transmembrane loops controlling  $K^+$  flux (Choe 2002). Additionally, this domain contains the typical Rossman fold motif (G–X–G–X–X–G...D) involved in NAD binding, indicating metabolic control of transporter function (Roosild et al. 2002; Jiang et al. 2001). KEA family remained relatively constant at 3–7 genes from unicellular algae to flowering plants suggesting conserved roles and its functions are largely unknown (Chanroj et al. 2012). The sole functional information of KEA protein in plants comes from the ATKEA2 which functions at chloroplast as a cation/proton exchanger with preference for  $K^+$  and maintains the pH homeostasis (Aranda-Sicilia et al. 2012). In this present study, AM1 was classified into the same clades (KEA1a) as the ATKEA2 (Chanroj et al. 2012), suggesting their similar functions, i.e., the similar targeting to the chloroplast and mainly leaf expression in AM1 to ATKEA2 (Fig. 5). More recently, A two-pore  $K^+$  channel which controls photosynthetic light utilization has been found to be located in the thylakoid membrane of Arabidopsis (Carraretto et al. 2013), and the more precise localization of AM1 need to be further investigated. Although we failed to test the cation transport activity of AM1, the up-regulation of AM1 expression levels by salt induction as well as the enhanced sensitivity to KCl at seed germination suggests that AM1 plays an important role in regulation of monovalent cation efflux to maintain the ion homeostasis in plant cells (Fig. 7).

Although bioinformatic analysis and proteomic studies suggested that KEA transporters in eukaryotes served functions mainly in the chloroplast or plastid of plant cells: firstly, up to date, all plants contained three subtypes of KEA from lower green algae to higher flowering plants (Chanroj et al. 2012); secondly, almost all the KEAs are found in plastid-containing organisms, ranging from cyanobacteria, green plants, red algae to secondary endosymbionts, but not in fungi; thirdly, some KEA1a proteins were previously identified in proteomic studies of the Arabidopsis chloroplast inner envelope (Ferro et al. 2010; Brautigam and Weber 2009; Zybailov et al. 2008). More recently, ATKEA2 was reported to target to chloroplasts in cotyledons (Aranda-Sicilia et al. 2012). Yet no genetic evidence and the phenotypic description of KEA mutants were provided to support this thesis. In our study, we isolated a KEA mutant designated *am1* by fine mapping. *Am1* mutant allele had a 2-bp deletion in 1th ORF and caused a premature stop codon which directly led to the loss of two

main functional domains (Figs. 3e, 4a). Thus, *am1* could be considered to lose most of the functions. *Am1* mutant allele displayed a chlorophyll-deficient phenotype and abnormal chloroplast ultrastructure (Figs. 1, 2). In addition, *am1* showed abnormal chloroplast gene expression and protein accumulation (Fig. 6). These findings provided the genetic evidence for KEA proteins involving in the chloroplast development. In the *am1* mutants, the accumulation of photosystem-II subunits and the values of key photosynthetic parameters were similar to the wild-type (Fig. 6b; Table S2), indicating that photosystem II apparatus was not impaired in *am1* mutant. Monovalent cation/proton antiporters controlling chloroplast development has been previously reported. The Arabidopsis *CHX23* gene encodes a putative  $Na^+$  ( $K^+$ )/ $H^+$  exchanger and functions in the adjustment of pH in the chloroplast and cytoplasm (Song et al. 2004). Leaves of *chx23* mutant displayed pale-yellow with higher cytosolic pH than wild-type. Although the mechanism for AM1 affecting the chloroplast development might differ from that in CHX23, it provided a cue for further investigating the roles of AM1 in chloroplast development.

Drought is one of the prime abiotic stresses in the world and poses a serious threat to plant growth and seed production. To survive, plants have to respond to and adapt to the stresses. One of strategies is the reduction of stomatal opening to prevent water from losing. Reactive oxygen species (ROS) including hydrogen peroxide ( $H_2O_2$ ) that were widely generated under various stress have been proposed to function as second messengers in abscisic acid (ABA) signaling in guard cells (McAinsh et al. 1996; Hamilton et al. 2000; Kohler et al. 2003; Bright et al. 2006; Zhang et al. 2001).  $H_2O_2$  can also induce stomata closure independent of ABA signaling pathway (Huang et al. 2009). In plants, lots of cation/proton antiporters have been reported to regulate salt tolerance (Chanroj et al. 2012). However, none was showed to participate in drought tolerance. In this study, we showed that AM1 was induced by PEG and the *am1* mutant plants could enhance the drought tolerance (Figs. 7a, 8a, b). Further analysis indicated that AM1 mutation resulted in a smaller stomatal opening and more accumulation of  $H_2O_2$  (Fig. 8c–e). Previous studies showed that chloroplasts were the site of ABA biosynthesis (Seo and Koshida 2002), and pigment-deficient mutants reduced endogenous level of ABA (Fambrini et al. 1993). Thus, increased stomatal closure in the *am1* mutant probably was not due to endogenous ABA accumulation. Over-accumulation of  $H_2O_2$  in *am1* mutant most likely acted as an initiator of increased stomatal closure to confer the drought tolerance.

In summary, we isolated and characterized the first KEA mutant in rice. Our results not only provided a genetic evidence that KEA involved in the chloroplast development,

but also revealed their novel function in the regulation of drought stress. However, it remains a challenge to identify their roles in ion transport and interpret molecular mechanism, as to how the AM1 affects the chloroplast development and drought stress.

**Acknowledgments** This work was supported by the National Natural Science Foundation of China (31000667), National Transgenic Science and Technology Program (2011ZX08009 003), and the Major State Basic Research Development Program of China (973 Program, 2009CB8500).

**Conflict of interest** The authors have declared that no conflict of interests exist.

## References

- Apel K, Hirt H (2004) Reactive oxygen species: metabolism, oxidative stress, and signal transduction. *Annu Rev Plant Biol* 55:373–399. doi:10.1146/annurev.arplant.55.031903.141701
- Aranda-Sicilia MN, Cagnac O, Chanroj S, Sze H, Rodriguez-Rosales MP, Venema K (2012) Arabidopsis KEA2, a homolog of bacterial KefC, encodes a K(+)/H(+) antiporter with a chloroplast transit peptide. *Biochim Biophys Acta* 1818(9):2362–2371. doi:10.1016/j.bbame.2012.04.011
- Archer EK, Bonnett HT (1987) Characterization of a virescent chloroplast mutant of tobacco. *Plant Physiol* 83(4):920–925
- Arnon DI (1949) Copper enzymes in isolated chloroplasts polyphenoloxidase in beta vulgaris. *Plant Physiol* 24(1):1–15
- Booth IR (2003) Bacterial ion channels. *Genet Eng (N Y)* 25:91–111
- Brautigam A, Weber AP (2009) Proteomic analysis of the proplastid envelope membrane provides novel insights into small molecule and protein transport across proplastid membranes. *Mol Plant* 2(6):1247–1261. doi:10.1093/mp/ssp070
- Bright J, Desikan R, Hancock JT, Weir IS, Neill SJ (2006) ABA-induced NO generation and stomatal closure in Arabidopsis are dependent on H<sub>2</sub>O<sub>2</sub> synthesis. *Plant J* 45(1):113–122. doi:10.1111/j.1365-313X.2005.02615.x
- Carraretto L, Formentin E, Teardo E, Checchetto V, Tomizioli M, Morosinotto T, Giacometti GM, Finazzi G, Szabo I (2013) A thylakoid-located two-pore K<sup>+</sup> channel controls photosynthetic light utilization in plants. *Science* 342(6154):114–118. doi:10.1126/science.1242113
- Chanroj S, Wang G, Venema K, Zhang MW, Delwiche CF, Sze H (2012) Conserved and diversified gene families of monovalent cation/H(+) antiporters from algae to flowering plants. *Front Plant Sci* 3:25. doi:10.3389/fpls.2012.00025
- Chen S, Tao L, Zeng L, Vega-Sanchez ME, Umemura K, Wang GL (2006) A highly efficient transient protoplast system for analyzing defence gene expression and protein–protein interactions in rice. *Mol Plant Pathol* 7(5):417–427. doi:10.1111/j.1364-3703.2006.00346.x
- Choe S (2002) Potassium channel structures. *Nat Rev Neurosci* 3(2):115–121. doi:10.1038/nrn727
- Dong H, Fei GL, Wu CY, Wu FQ, Sun YY, Chen MJ, Ren YL, Zhou KN, Cheng ZJ, Wang JL, Jiang L, Zhang X, Guo XP, Lei CL, Su N, Wang H, Wan JM (2013) A rice virescent-yellow leaf mutant reveals new insights into the role and assembly of plastid caseinolytic protease in higher plants. *Plant Physiol* 162(4):1867–1880. doi:10.1104/pp.113.217604
- Emanuelsson O, Nielsen H, von Heijne G (1999) ChloroP, a neural network-based method for predicting chloroplast transit peptides and their cleavage sites. *Protein Sci* 8(5):978–984. doi:10.1110/ps.8.5.978
- Fambrini M, Pugliesi C, Vernieri P, Giuliano G, Baroncelli S (1993) Characterization of a sunflower (*Helianthus annuus* L.) mutant, deficient in carotenoid synthesis and abscisic-acid content, induced by in vitro tissue culture. *Theor Appl Genet* 87(1–2):65–69. doi:10.1007/BF00223746
- Ferro M, Brugiere S, Salvi D, Seigneurin-Berny D, Court M, Moyet L, Ramus C, Miras S, Mellal M, Le Gall S, Kieffer-Jaquinod S, Bruley C, Garin J, Joyard J, Masselon C, Rolland N (2010) AT\_CHLORO, a comprehensive chloroplast proteome database with subplastidial localization and curated information on envelope proteins. *Mol Cell Proteomics* 9(6):1063–1084. doi:10.1074/mcp.M900325-MCP200
- Finn RD, Mistry J, Tate J, Coghill P, Heger A, Pollington JE, Gavin OL, Gunasekaran P, Ceric G, Forslund K, Holm L, Sonnhammer EL, Eddy SR, Bateman A (2010) The Pfam protein families database. *Nucleic Acids Res* 38:D211–D222. doi:10.1093/nar/gkp985
- Hamilton DW, Hills A, Kohler B, Blatt MR (2000) Ca<sup>2+</sup> channels at the plasma membrane of stomatal guard cells are activated by hyperpolarization and abscisic acid. *Proc Natl Acad Sci USA* 97(9):4967–4972. doi:10.1073/pnas.080068897
- Hiei Y, Ohta S, Komari T, Kumashiro T (1994) Efficient transformation of rice (*Oryza sativa* L.) mediated by Agrobacterium and sequence analysis of the boundaries of the T-DNA. *Plant J* 6(2):271–282
- Holtorf H, Apel K (1996) Transcripts of the two NADPH protochlorophyllide oxidoreductase genes *PorA* and *PorB* are differentially degraded in etiolated barley seedlings. *Plant Mol Biol* 31(2):387–392
- Huang XY, Chao DY, Gao JP, Zhu MZ, Shi M, Lin HX (2009) A previously unknown zinc finger protein, DST, regulates drought and salt tolerance in rice via stomatal aperture control. *Genes Dev* 23(15):1805–1817. doi:10.1101/gad.1812409
- Hwang SR, Tabita FR (1989) Cloning and expression of the chloroplast-encoded *rbcL* and *rbcS* genes from the marine diatom *Cylindrotheca* sp. strain N1. *Plant Mol Biol* 13(1):69–79
- Jiang Y, Pico A, Cadene M, Chait BT, MacKinnon R (2001) Structure of the RCK domain from the *E. coli* K<sup>+</sup> channel and demonstration of its presence in the human BK channel. *Neuron* 29(3):593–601
- Jung KH, Hur J, Ryu CH, Choi Y, Chung YY, Miyao A, Hirochika H, An G (2003) Characterization of a rice chlorophyll-deficient mutant using the T-DNA gene-trap system. *Plant Cell Physiol* 44(5):463–472
- Kohler B, Hills A, Blatt MR (2003) Control of guard cell ion channels by hydrogen peroxide and abscisic acid indicates their action through alternate signaling pathways. *Plant Physiol* 131(2):385–388. doi:10.1104/pp.016014
- Kumar AM, Soll D (2000) Antisense HEMA1 RNA expression inhibits heme and chlorophyll biosynthesis in Arabidopsis. *Plant Physiol* 122(1):49–56
- Kusumi K, Sakata C, Nakamura T, Kawasaki S, Yoshimura A, Iba K (2011) A plastid protein NUS1 is essential for build-up of the genetic system for early chloroplast development under cold stress conditions. *Plant J* 68(6):1039–1050. doi:10.1111/j.1365-313X.2011.04755.x
- Maser P, Thomine S, Schroeder JI, Ward JM, Hirschi K, Sze H, Talke IN, Amtmann A, Maathuis FJ, Sanders D, Harper JF, Tchiew J, Gribskov M, Persans MW, Salt DE, Kim SA, Guerinet ML (2001) Phylogenetic relationships within cation transporter families of Arabidopsis. *Plant Physiol* 126(4):1646–1667
- Matsuoka M (1990) Classification and characterization of cDNA that encodes the light-harvesting chlorophyll *a/b* binding protein of photosystem II from rice. *Plant Cell Physiol* 31(4):519–526

- McAinsh MR, Clayton H, Mansfield TA, Hetherington AM (1996) Changes in stomatal behavior and guard cell cytosolic free calcium in response to oxidative stress. *Plant Physiol* 111(4):1031–1042
- Rodermel S (2001) Pathways of plastid-to-nucleus signaling. *Trends Plant Sci* 6(10):471–478
- Roosild TP, Miller S, Booth IR, Choe S (2002) A mechanism of regulating transmembrane potassium flux through a ligand-mediated conformational switch. *Cell* 109(6):781–791
- Seo M, Koshiba T (2002) Complex regulation of ABA biosynthesis in plants. *Trends Plant Sci* 7(1):41–48
- Song CP, Guo Y, Qiu Q, Lambert G, Galbraith DW, Jagendorf A, Zhu JK (2004) A probable Na<sup>+</sup> (K<sup>+</sup>)/H<sup>+</sup> exchanger on the chloroplast envelope functions in pH homeostasis and chloroplast development in *Arabidopsis thaliana*. *Proc Natl Acad Sci USA* 101(27):10211–10216. doi:10.1073/pnas.0403709101
- Su N, Hu ML, Wu DX, Wu FQ, Fei GL, Lan Y, Chen XL, Shu XL, Zhang X, Guo XP, Cheng ZJ, Lei CL, Qi CK, Jiang L, Wang H, Wan JM (2012) Disruption of a rice pentatricopeptide repeat protein causes a seedling-specific albino phenotype and its utilization to enhance seed purity in hybrid rice production. *Plant Physiol* 159(1):227–238. doi:10.1104/pp.112.195081
- Sugimoto H, Kusumi K, Tozawa Y, Yazaki J, Kishimoto N, Kikuchi S, Iba K (2004) The virescent-2 mutation inhibits translation of plastid transcripts for the plastid genetic system at an early stage of chloroplast differentiation. *Plant Cell Physiol* 45(8):985–996. doi:10.1093/pcp/pch111
- Sugimoto H, Kusumi K, Noguchi K, Yano M, Yoshimura A, Iba K (2007) The rice nuclear gene, VIRESCENT 2, is essential for chloroplast development and encodes a novel type of guanylate kinase targeted to plastids and mitochondria. *Plant J* 52(3):512–527. doi:10.1111/j.1365-313X.2007.03251.x
- ThordalChristensen H, Zhang Z, Wei Y, Collinge D (1997) Subcellular localization of H<sub>2</sub>O<sub>2</sub> in plants. H<sub>2</sub>O<sub>2</sub> accumulation in papillae and hypersensitive response during the barley–powdery mildew interaction. *Plant J* 11(6):1187–1194
- Wu Z, Zhang X, He B, Diao L, Sheng S, Wang J, Guo X, Su N, Wang L, Jiang L, Wang C, Zhai H, Wan J (2007) A chlorophyll-deficient rice mutant with impaired chlorophyllide esterification in chlorophyll biosynthesis. *Plant Physiol* 145(1):29–40. doi:10.1104/pp.107.100321
- Yoo SC, Cho SH, Sugimoto H, Li J, Kusumi K, Koh HJ, Iba K, Paek NC (2009) Rice virescent3 and stripe1 encoding the large and small subunits of ribonucleotide reductase are required for chloroplast biogenesis during early leaf development. *Plant Physiol* 150(1):388–401. doi:10.1104/pp.109.136648
- Zhang X, Zhang L, Dong F, Gao J, Galbraith DW, Song CP (2001) Hydrogen peroxide is involved in abscisic acid-induced stomatal closure in *Vicia faba*. *Plant Physiol* 126(4):1438–1448
- Zhang H, Li J, Yoo JH, Yoo SC, Cho SH, Koh HJ, Seo HS, Paek NC (2006) Rice Chlorina-1 and Chlorina-9 encode ChlD and ChlI subunits of Mg-chelatase, a key enzyme for chlorophyll synthesis and chloroplast development. *Plant Mol Biol* 62(3):325–337. doi:10.1007/s11103-006-9024-z
- Zhou K, Ren Y, Lv J, Wang Y, Liu F, Zhou F, Zhao S, Chen S, Peng C, Zhang X, Guo X, Cheng Z, Wang J, Wu F, Jiang L, Wan J (2013) Young leaf chlorosis 1, a chloroplast-localized gene required for chlorophyll and lutein accumulation during early leaf development in rice. *Planta* 237(1):279–292. doi:10.1007/s00425-012-1756-1
- Zimmermann P, Hirsch-Hoffmann M, Hennig L, Gruissem W (2004) Genevestigator. *Arabidopsis* microarray database and analysis toolbox. *Plant Physiol* 136(1):2621–2632. doi:10.1104/pp.104.046367
- Zybailov B, Rutschow H, Friso G, Rudella A, Emanuelsson O, Sun Q, van Wijk KJ (2008) Sorting signals, N-terminal modifications and abundance of the chloroplast proteome. *PLoS One* 3(4):e1994. doi:10.1371/journal.pone.0001994